第 30 回日本バーチャルリアリティ学会大会論文集（2025 年 9 月）

A Wearable Olfactory Display: Driving Circuit Optimization for Supplying Fragrances

Zhe ZOU[1)], Takamichi NAKAMOTO[1)], Shoichi HASEGAWA[1)]

1) Institute of Sciency Tokyo（〒 226-8501 4259, Nagatsuta-cho, Midori-ku, Yokohama, zou.z.aa@m.titech.ac.jp）

Abstract: We introduce a wearable olfactory display for VR applications that achieves precise odor dispensing using micro dispensers and electroosmotic pumps. The system's control signals and driving circuits were optimized to ensure reliable operation. The performance of individual subsystems was validated through sensor-based tests, and the integrated prototype's effectiveness was assessed within a custom smell-enhanced VR application via user evaluation. This work demonstrates the device's potential for creating more immersive human-computer interaction.

Keywords： Wearable olfactory display, Electroosmotic pump, Micro dispenser, Circuit design

1. Introduction

While visual, auditory, and haptic technologies are well-established in the field of virtual reality (VR), the integration of olfaction remains a key challenge for creating truly multisensory user experiences, particularly for wearable devices [1]. Many existing wearable olfactory displays rely on a single type of dispensing component for the liquid fragrances, such as a heater or a micro dispenser [2, 3]. Although they are compact, they often lack a flexible fragrance supplying function, which is indispensable for precisely controlling the perceived intensity of a scent.

To achieve more flexible control, state-of-the-art systems often integrate more advanced fluidic components, like electroosmotic (EO) pumps, to precisely regulate the liquid supply pressure and flow rate [4]. However, their driving circuits are typically bulky for wearable device, and suffer from overheating during the demanding operation. This has leaves a critical gap in the olfactory display: a device that is both wearable and capable of precise, intensive dispensing [5].

This paper addresses this gap directly by presenting a wearable olfactory display that integrates both EO pumps and micro dispensers, supported by a compact, high-voltage pulse width modulation (PWM) circuit and a novel, power-efficient h-type signal driver, respectively. We validated our system through a series of quantitative and qualitative evaluations. Component-level tests confirmed its flexible control and a significant reduction in heat generation. A user evaluation within a customized VR application demonstrated the system's effectiveness in creating an immersive, scent-enhanced experience, confirming the viability of our approach for practical, wearable HCI applications.

2. Fragrance supply

2.1 System schematic

The architecture of the proposed olfactory display, depicted in Fig 1, is organized into three primary subsystems: control, odor dispensing, and odor delivery. The core of the device is the odor dispensing part, which features multiple parallel channels. Each channel is individually equipped with an EO pump (EBP-RF1R, Takasago Electric Company) and a micro dispenser (INKA2438510H, The Lee Company), enabling the precise dispensing of different fragrances to a shared odor generation unit. A forced airflow then directs the generated scent to the user. The entire system is controlled by an FPGA-based control board according to the commands from the computer.

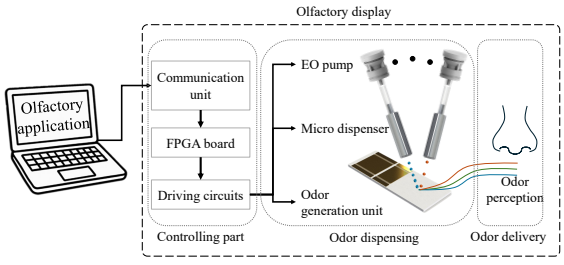

Fig 1: Schematic of the olfactory display system.

2.2 Electroosmotic pump

The EO pump is a low-speed pump that provides a stable supply of liquid based on the electroosmotic effect, as illustrated in Fig 2. A negatively charged porous membrane divides the interior into two cavities. During the idle state, the fragrance is stored in the upper side and its positively charged ions are attracted to the membrane

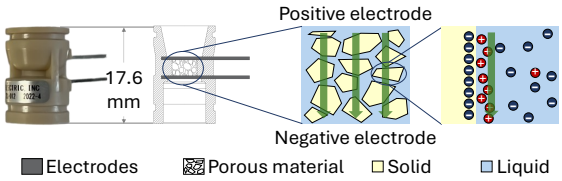

Fig 2: The internal structure of the EO pump and the principle of the electroosmotic effect.

surface. When an electric field is generated by an external voltage, these positive ions travel toward the cathode through the porous membrane, dragging the surrounding bulk liquid with them. Consequently, the liquid flow is generated, which can be regulated by adjusting the applied voltage.

2.3 Micro dispenser

The system employs a solenoid-based micro dispenser connected to the EO pump, which can eject liquid via the reciprocating motion of an internal plunger. As illustrated in Fig 3, applying a voltage to the coil can retract the plunger against a spring, forming a space in front of the plunger to let the liquid fill in. When the voltage is removed, the spring's restoring force pushes the plunger forward, rapidly ejecting a tiny droplet through the orifice. By matching the flow rate from the EO pump and the ejection frequency, the overall dispensing volume is accurately controlled in nanoliter level.

3. Driving circuit

3.1 Voltage modulation of EO pump

Flexibly adjusting the flow rate of the EO pump requires a wide voltage range higher than 24 V (power supply voltage) in most case. Therefore, a two-stage voltage modulation circuit was developed. First, a DC-DC converter (MHV12-300S10P, Bellnix Co. Ltd.) steps up the input voltage to 250 V. Then, a PWM circuit, shown in Fig 4, controls the equivalent voltage applied to the pump ranging from 0 to 200 V using a high-voltage SSR (AQW210S, Panasonic Semiconductor). Considering both the turn on (0.23ms typ.) and turn off (0.04ms typ.) time of the SSR, and the rapid response of the output voltage, the PWM repetition cycle was determined as 5ms. This PWM approach was chosen over conventional digital to analog converter-based (DAC-based) solutions for its superior compactness and cost-effectiveness [4].

Additionally, because the EO pump has inherent capacitance, a parallel bleeder resistor is included. This component provides a discharge path for stored charge when the SSR is in its off-state, ensuring the voltage falls sharply to zero. This capability is essential for the precise temporal control of the pump's operation.

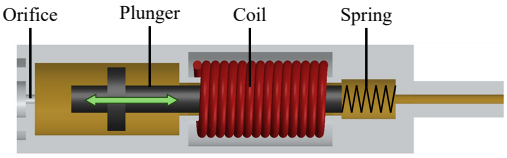

Fig 3: Internal structure and operating principle of the solenoid micro dispenser.

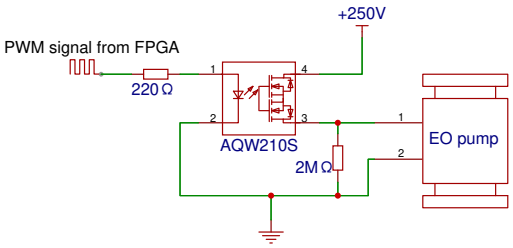

Fig 4: Schematic of the custom PWM circuit for driving the EO pump.

3.2 h-type signal for micro dispenser

The conventional method for driving the micro dispenser uses a constant 24 V pulse for the entire actuation cycle. While this approach is functional, it causes significant resistive heating at high ejection frequencies, which compromises the device's stability during prolonged operation. To mitigate this thermal issue, we developed a triphasic driving signal: termed the h-type signal. This signal consists of a brief, high-voltage (24 V) actuation phase to retract the plunger, immediately followed by a low-voltage (5 V) holding phase that maintains the plunger's position using minimal energy, as well as a zero-voltage state to release the plunger. By lowering the voltage during the non-critical holding period, this strategy reduces unnecessary power consumption.

The h-type signal is generated by the driving circuit shown in Fig 5. This circuit uses two parallel-connected, PMOS-based switching stages to generate the 24 V and 5 V levels, with each stage governed by a control signal from an FPGA individually. The two voltage outputs are combined through a Schottky diode, which allows the higher voltage to dominate the final output. During the high-voltage phase, both stages are enabled, but the diode blocks the 5 V output, ensuring a clean 24 V output. For the low-voltage phase, the 24 V stage is deactivated, allowing the 5 V output to automatically conduct through the diode. This electric design ensures smooth transitions between the two voltage phases.

Additionally, as the micro dispenser's coil is an inductive load, a flywheel diode is placed in parallel with it. This provides a safe path for current to recirculate when the coil is de-energized, suppressing potentially damaging voltage spikes and protecting the PMOS switches.

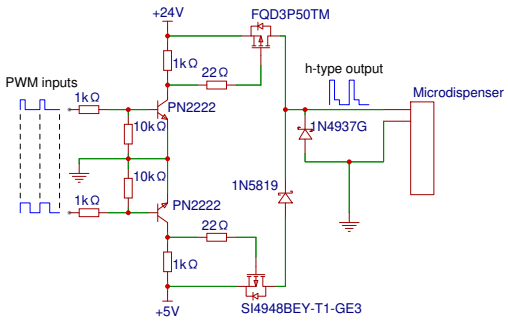

Fig 5: The h-type signal driver, featuring dual PMOS switches for the triphasic output and a flywheel diode for inductive load protection.

4. Evaluation

4.1 Flow rate regulation

While preliminary tests confirmed that the PWM driving circuit's output voltage accurately tracked the target setpoint (with <1.5% error), it is necessary to validate that this electrical strategy achieves a reliable and linear regulation of the EO pump's practical fluidic flow rate.

The flow rate of the EO pump was measured indirectly using a high-resolution digital balance (AUX320, SHIMADZU CORPORATION), as depicted in Fig 6. During trials, the EO pump delivered pure ethanol, which is a commonly used solvent for fragrances, into a collection bottle placed on the balance. To minimize mass loss from evaporation, the bottle's opening was covered with parafilm, leaving a small aperture that is just large enough for the dispensed droplets to pass through. Furthermore, the bottle was pre-filled with a small amount of ethanol to maintain a constant evaporative surface area throughout the experiment.

The EO pump was operated at voltages ranging from 10 V to 200 V in 10 V increments. Each voltage level was tested in three 15-minute trials, with a 3-minute interval between each trial. The mass of dispensed liquid was determined by recording the weight change on the balance. To correct for evaporative losses, three identical trials were also conducted under zero-voltage. The mass lost to evaporation during these 0 V trials was then added to the measured mass gain from other trials to yield the corrected total dispensed mass. From this corrected data, the average flow rate for each driving voltage was calculated and is illustrated in Fig 7.

As shown in Fig 7, the measured flow rate exhibits a strong linear dependence on the applied voltage. The repeatability of the measurement was high, with the coefficient of variation (n = 3) for most data points under 17% except the data at 20 V. It is confirmed that the

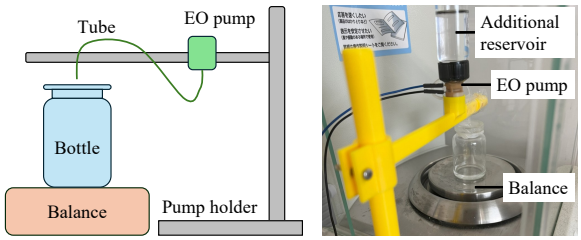

Fig 6: Experiment setup to measure the EO pump flow rate.

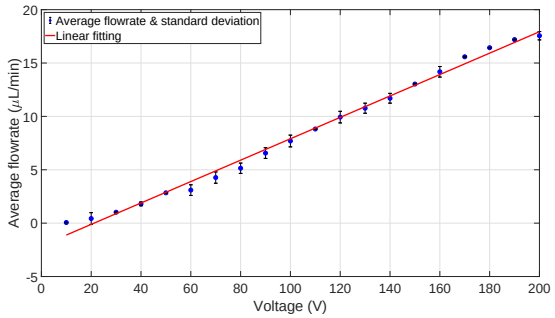

Fig 7: Measured EO pump flow rate as a function of the applied driving voltage.

EO pump driving circuit provides highly stable and predictable control over the flow rate.

4.2 Ejection performance of micro dispenser

We validated the performance of the h-type signal, first confirming its successful generation with an oscilloscope (Fig 8). The micro dispenser demonstrated robust operation across a wide frequency range of 0-400 Hz.

Additionally, in comparative tests at 100 Hz, the h-type signal reduced temperature rising by 42.7% over a 6-minute period compared to a conventional pulse signal, as measured by an infrared thermometer (THI-301S, TASCO). This significant reduction in thermal load extends the device's capacity for continuous operation, directly addressing a key limitation in long-duration, scent-enabled virtual experiences.

4.3 User evaluation

To gather preliminary feedback on the device's real-world performance, we held several demonstration sessions with a custom-developed, smell-enhanced VR application. In the application, users could interact with various virtual objects to trigger corresponding olfactory stimuli alongside visual and auditory feedback (Fig 9).

Following the experience, we collected informal, text-based comments from participants (examples shown in Fig 10). A summary of this qualitative feedback exhibits positive assessment. Most participants reported that they could successfully perceive and differentiate between the various odors, and many commented on an en-

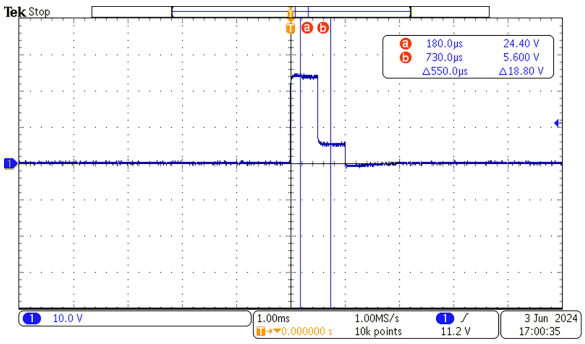

Fig 8: The generated triphasic h-type signal. Cursors are used to highlight the representative voltage levels of the 24 V and 5 V phases.

Fig 9: Participant wears the olfactory display and explores the scent objects.

hanced sense of immersion. However, some comments also noted difficulty in perceiving certain odors, which may be attributable to individual differences in olfactory sensitivity or a lack of familiarity with the specific scents used. While not a formal controlled study, this positive initial feedback suggests that our odor dispensing strategy is effective and has strong potential to improve user immersion in interactive virtual environments.

5. Conclusion

In this paper, we proposed an effective odor dispensing strategy for a wearable olfactory display. Customized driving signals and circuits were developed to achieve stable and rapid control of the dispensing electronics. A series of quantitative tests demonstrated that the proposed methodology yields reliable and repeatable performance, laying the groundwork for future advancements in olfactory display technology. Furthermore, a user evaluation within a smell-enhanced VR application supported the practical viability of our method for enhancing immersive experiences. As a next step, we will focus on optimizing the circuit design to further reduce its physical

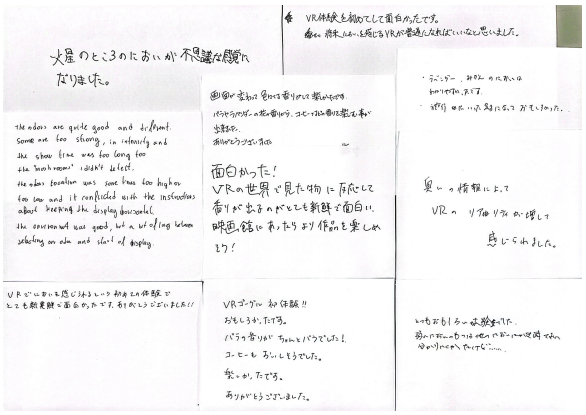

Fig 10: User comments on the performance of the proposed olfactory display, collected from demonstration at our campus opening event.

size. This will involve developing custom components to make the device more suitable for wearable applications while maintaining its high performance.

Acknowledgement

We wish to thank Mr. Hsueh Han Wu, Mr. Sungho Lee, Dr. Kelvin Cheng of Rakuten mobile for making the smell-enhanced VR application.

This work was in part supported by JST Mirai project (JPMJMI25G1).

References

[1] Jordan Tewell and Nimesha Ranasinghe. A review of olfactory display designs for virtual reality environments. *ACM Computing Surveys*, 56(11):1–35, 2024.

[2] Xiang Fei, Yanan Wang, Yucheng Li, Zhengyu Lou, Yifan Yan, Yujing Tian, and Qingjun Chen. Odorcarousel: A design tool for customizing smell-enhanced virtual experiences. *International Journal of Human–Computer Interaction*, 41(4):2089–2104, 2025.

[3] Takamichi Nakamoto, Tatsuya Hirasawa, and Yukiko Hanyu. Virtual environment with smell using wearable olfactory display and computational fluid dynamics simulation. In *2020 IEEE Conference on Virtual Reality and 3D User Interfaces (VR)*, pages 713–720. IEEE, 2020.

[4] Hiroto Hayashi, Dani Prasetyawan, Masaaki Iseki, and Takamichi Nakamoto. Demo of odor reproduction using 20-component olfactory display. In *ICAT-EGVE (Posters and Demos)*, pages 45–46, 2022.

[5] Zhe Zou, Dani Prasetyawan, Hsueh Han Wu, Kelvin Cheng, and Takamichi Nakamoto. Extension of wearable olfactory display for multisensory vr experience. In *ICAT-EGVE (Paper)*. The Eurographics Association, 2024.